SURVIVAL PROBABILITY AT HIGH ENERGY

Errol Gotsman

Tel Aviv University

Outline

- A BRIEF INTRODUCTION TO RAPGAPS
- EXAMPLE OF SOFT SCATTERING MODEL
  GLM Model
- CALCULATION OF SURVIVAL PROBABILITY
- HARD MATRIX ELEMENT
- COMPILATION OF RESULTS FOR $< |S^2| >$

Examples of Rapidity Gaps

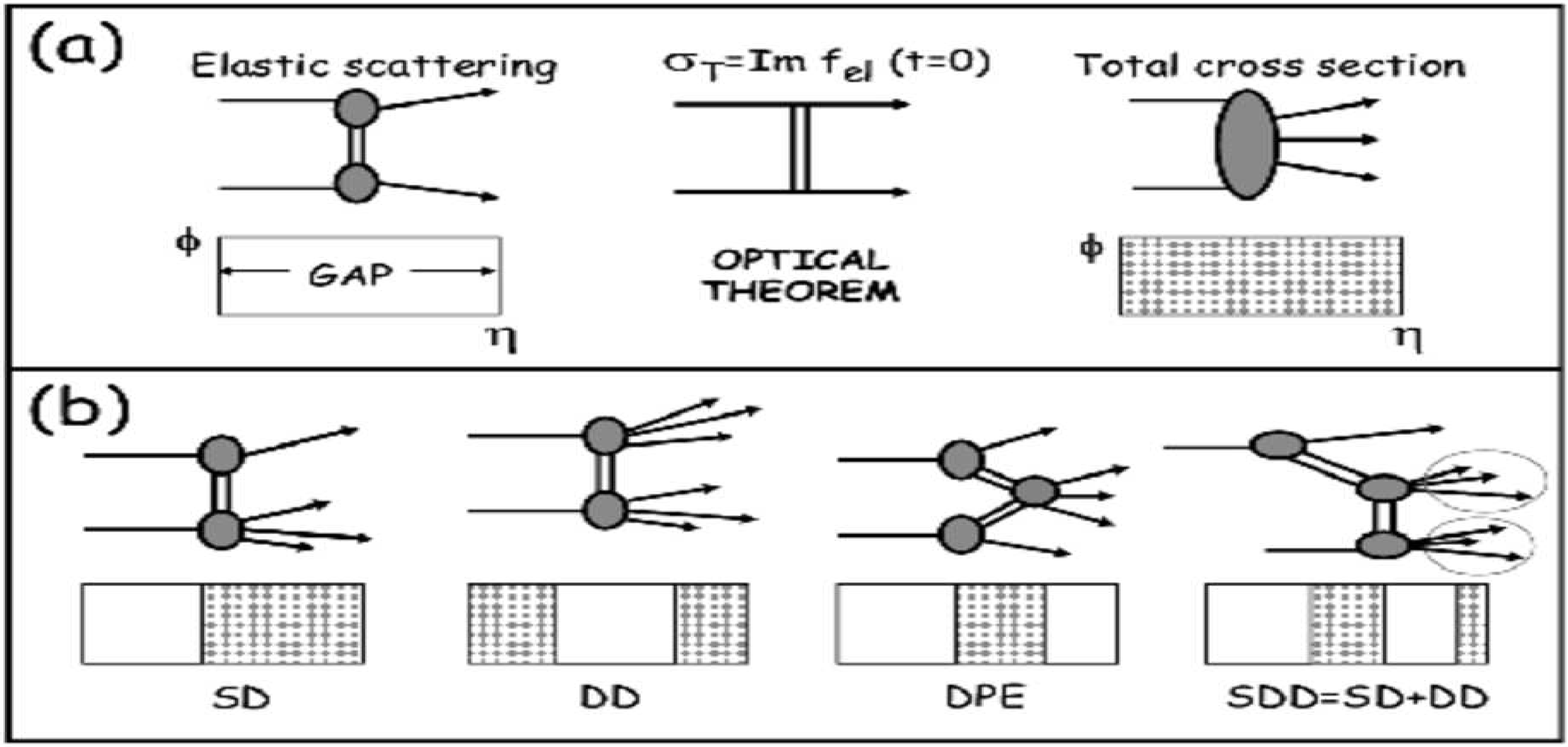

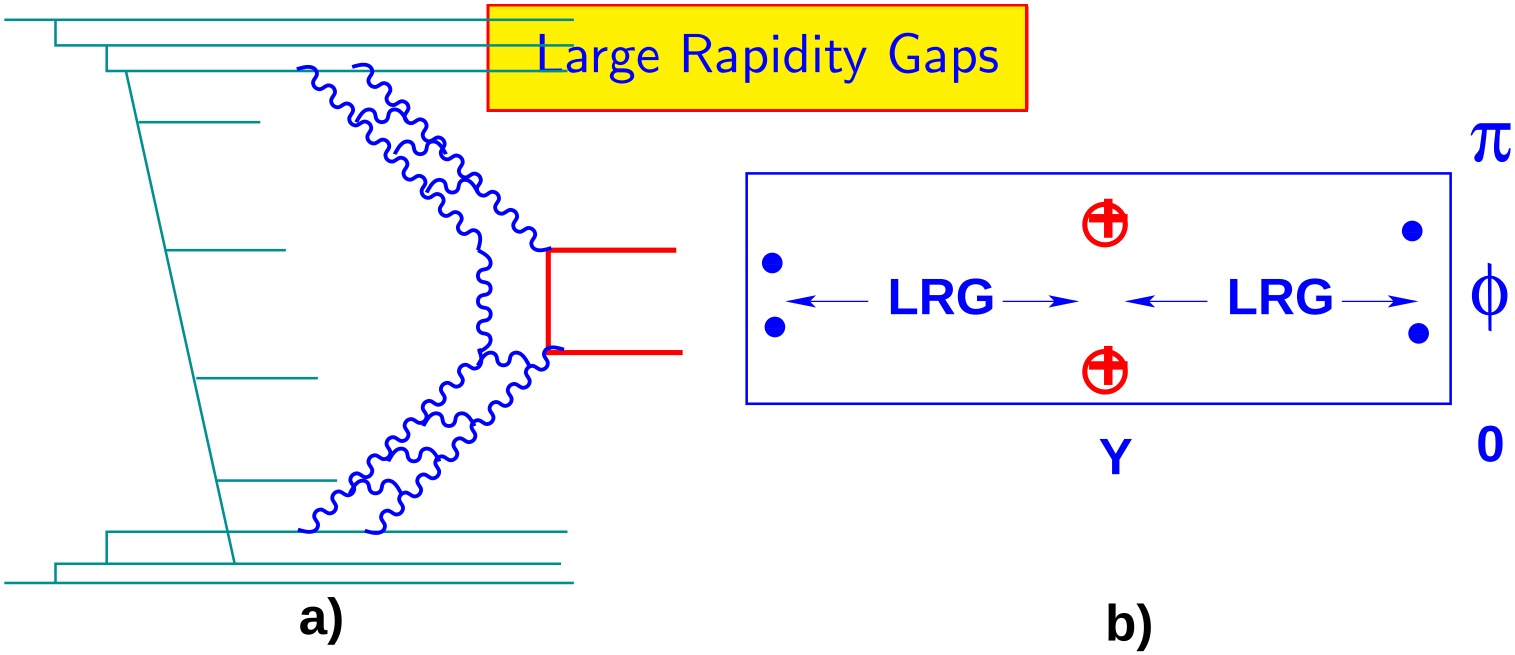

Soft rescattering between "partons" produce secondaries which may fill the rapidity gap (a), and (b) the lego-plot of our process.
The probability that there is no additional soft interactions, as shown in (a), gives the Survival Probability for the diffractive production.

Large Rapidity Gaps (LRG)

- LRG are expected whenever we have a process where a colour singlet is exchanged in the t channel.
- Historically, both Dokshitzer, Khoze and Troyan, AND Bjorken , suggested utilizing rapidity gaps as a signature for Higgs production, in the W-W fusion process in hadron-hadron collisions.
- Following Bjorken's notation : The fraction of events for which a LRG is expected, is the product of two factors.

$$f_{gap} = <\mid S \mid^2> \cdot F_s$$

1) $<\mid S \mid^2>$ denotes the survival probability, i.e. the fraction of events for which the spectator interactions do not fill the rapidity gap of interest.

2) F_s is the fraction of events due to t-channel singlet exchange.

- Bjorken by comparing the rate for the exchange of two gluons, in a colour singlet state, to the exchange of one gluon in a colour octet state, estimated F_s to be about 15 %.

Pictorial definition of $<|\, S \,|^2>$

$$f_{gap} = \frac{\sigma(\mathrm{LRG})}{\sigma(\mathrm{INCL})} = <S^2>$$

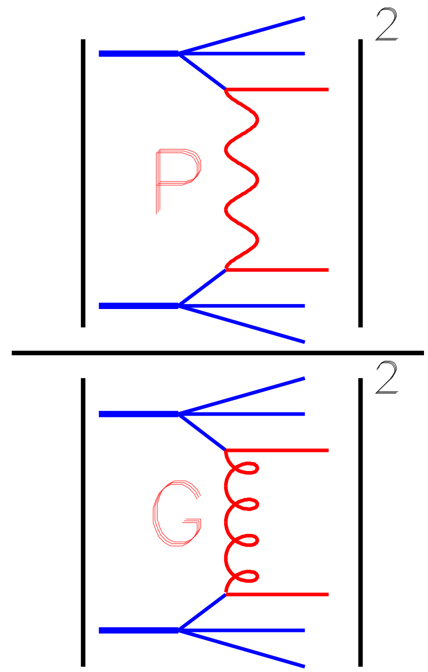

Experimental definition of LRG

- Experimentalists use a more practical definition of f_{gap}. At the Tevatron f_{gap} for LRG is defined to be the ratio:

$$f_{gap} = \frac{cross \;\; section \;\; for \;\; dijet \;\; production \;\; with \;\; LRG}{inclusive \;\; cross \;\; section \;\; for \;\; dijet \;\; production}$$

The jets are required to have a transverse energy $E_T^{jet} > \; 12 \; GeV$ at DO, and $E_T^{jet} > 20 \; GeV$ at CDF.

General Properties of $<|S^2|>$

- A more apt name for $<|S^2|>$ would be "suppression factor" of a hard process accompanied by a rapgap.

- It depends on the probability for the initial state to survive, and is sensitive to the spatial distribution of partons in the incoming hadrons. i.e. on the dynamics of the diffractive part of the scattering matrix.

- $<|S^2|>$ is not universal, but depends on the particular hard process, as well as the kinematic configuration.

- $<|S^2|>$ depends on the nature of the colour singlet ($I\!\!P$,W/Z or γ) exchange which generates the rapgap, as well as the distribution of partons inside the proton in impact parameter space.

Diffractive dijet production and diffractive DIS (KKMR)

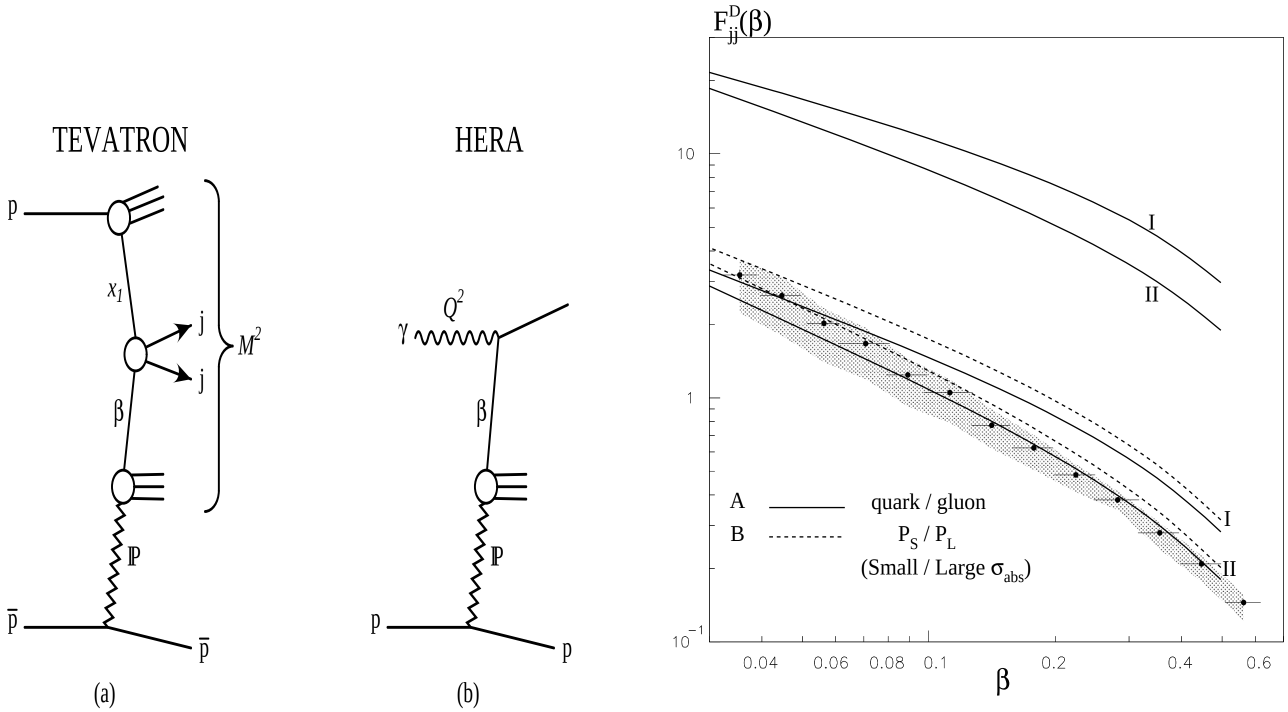

(c) The predictions for diffractive dijet production at the Tevatron, obtained from two alternative sets of 'HERA' diffractive parton distributions I and II compared with the CDF data. The upper two curves correspond to the neglect of ($< S^2 >$) "rescattering corrections", whereas the lower four curves show the effect of including these corrections using model A (continuous curves) and model B (dashed curves) for the diffractive eigenstates.

Calculation of $< |S|^2 >$ for Rapidity Gaps

- Depends on a parametrization of "soft" Pomeron (model dependent).
- Rescattering process ("screening or "absorption") is usually approximated by eikonal type model
- These models which include multi-Pomeron exchange, satisfy general principles of Unitarity (Froissart bound)
- Multi-Pomeron interactions are crucial in diffractive production (soft and hard)
- Parametrization of Hard Scattering Process.

GLM Formalism 1

Unitarity constraints:

$$Im\, T_{i,k}\,(s,b) = |T_{i,k}\,(s,b)\,|^2 + G^{in}_{i,k}(s,b)$$

A simple solution to the above equation is: $T_{i,k}(s,b) = i\left(1 - \exp\left(-\frac{\Omega_{i,k}(s,b)}{2}\right)\right)$,

where $\Omega_{i,k}(s,b)$ is the opacity.

Since the opacity increases with energy, the number of multiple interactions, $N \propto \Omega_{i,k}(s,b)$ grows (at larger optical density, we have a larger probability of interactions), leading to a smaller $<|S^2|>$.

$P^S_{i,k} = \exp\left(-\Omega_{i,k}(s,b)\right)$ is the probability that the initial projectiles (i,k) reach the final state interaction unchanged, regardless of the initial state rescatterings, (i.e. no inelastic interactions).

$$T_{ik} \;=\; 1 - e^{-\Omega_{ik}/2} \;=\; \sum$$

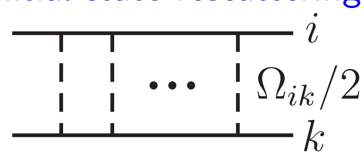

$$\Omega_{ik}/2 \;=$$

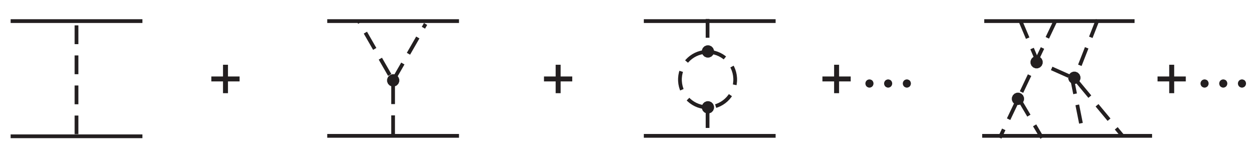

Examples of Pomeron diagrams

leading to diffraction NOT included in G-W mechanism

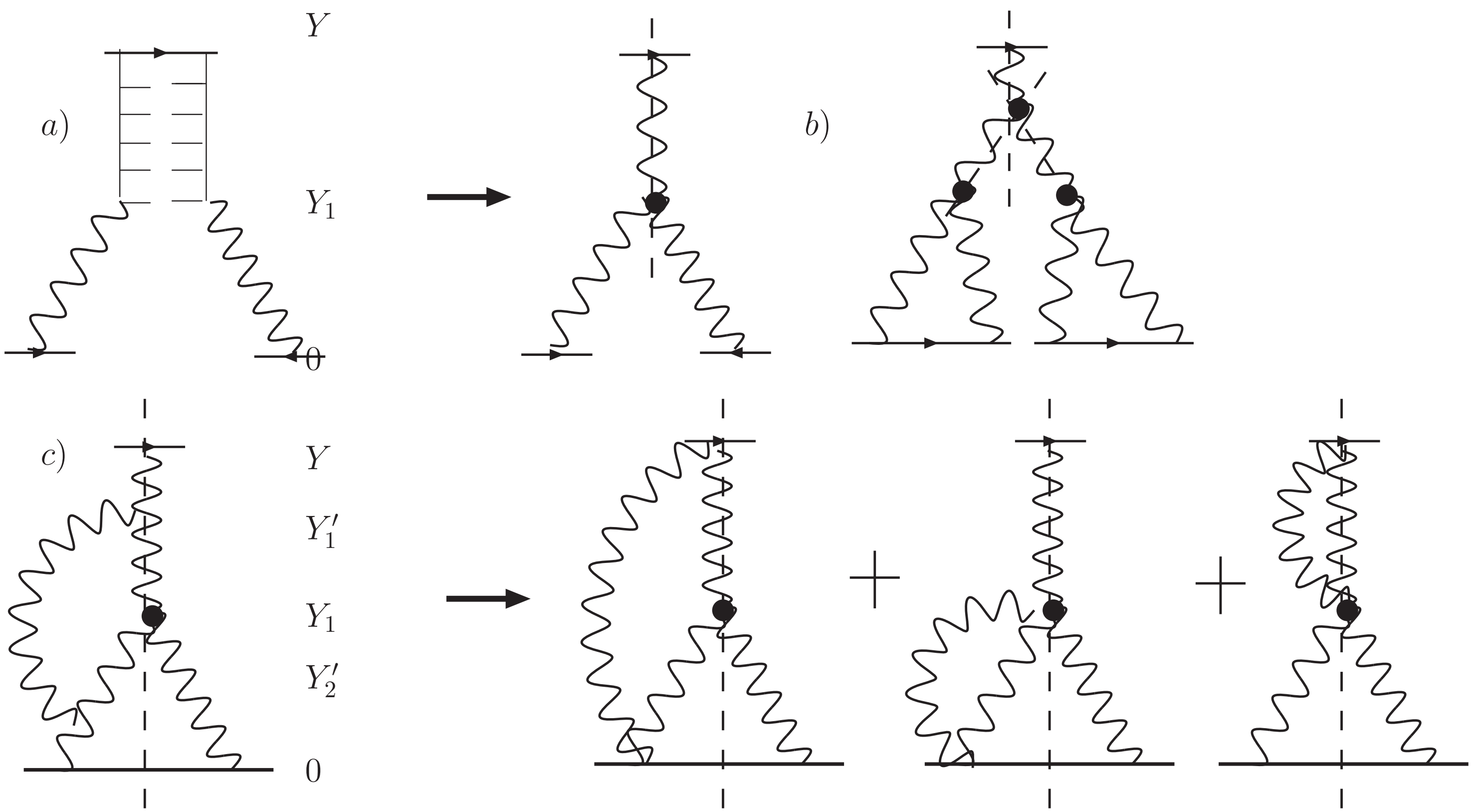

Examples of the Pomeron diagrams that lead to a different source of the diffractive dissociation that cannot be described in the framework of the G-W mechanism. (a) is the simplest diagram that describes the process of diffraction in the region of large mass $Y - Y_1 = \ln(M^2/s_0)$. (b) and (c) are examples of more complicated diagrams in the region of large mass. The dashed line shows the cut Pomeron, which describes the production of hadrons.

Example of enhanced and semi-enhanced diagram

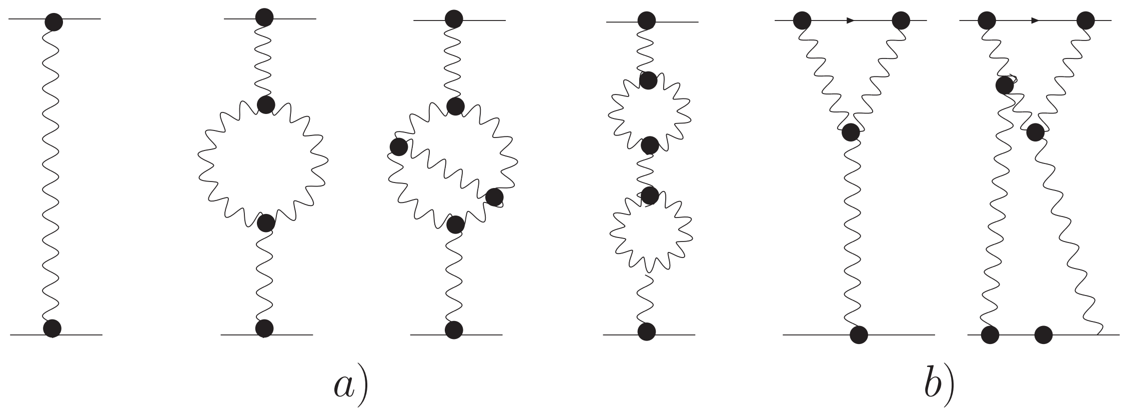

Different contributions to the Pomeron Green's function
a) examples of enhanced diagrams ;
(occur in the renormalisation of the Pomeron propagator)
b) examples of semi-enhanced diagrams
(occur in the renormalisation of the $I\!P$ -p vertex)
Multi-Pomeron interactions are crucial for the production of LARGE MASS DIFFRACTION

GLM Formalism 2

The input opacity $\Omega_{i,k}(s,b)$ corresponds to an exchange of a single bare Pomeron.

$$\Omega_{i,k}(s,b) \;=\; g_i(b)\, g_k(b)\, P(s). \qquad (1)$$

$P(s) \;=\; s^{\Delta_{I\!P}}$ and $g_i(b)$ is the Pomeron-hadron vertex parameterized in the form:

$$g_i\,(b) \;=\; g_i\, S_i(b) \;=\; \frac{g_i}{4\pi}\, m_i^3\, b\, K_1\,(m_i b)\,. \qquad (2)$$

$S_i(b)$ is the Fourier transform of $\frac{1}{(1+q^2/m_i^2)^2}$, where, q is the transverse momentum carried by the Pomeron.

The Pomeron's Green function that includes all enhanced diagrams is approximated using the MPSI procedure, in which a multi Pomeron interaction (taking into account only triple Pomeron vertices) is approximated by large Pomeron loops of rapidity size of $\ln s$.

$$G_{I\!P}\,(Y) \;=\; 1 \;-\; \exp\left(\frac{1}{T\,(Y)}\right)\frac{1}{T\,(Y)}\,\Gamma\left(0, \frac{1}{T\,(Y)}\right), \qquad (3)$$

where $T\,(Y) \;=\; \gamma\, e^{\Delta_{I\!P} Y}$ and $\Gamma\,(0, 1/T)$ is the incomplete gamma function.

Values of Parameters for our updated version

$\Delta_{I\!P}$	β	$\alpha'_{I\!P}(GeV^{-2})$	$g_1\,(GeV^{-1})$	$g_2\,(GeV^{-1})$	m_1 (GeV)	m_2 (GeV)
0.23	0.46	0.028	1.89	61.99	5.045	1.71
$\Delta_{I\!R}$	γ	$\alpha'_{I\!R}\,(GeV^{-2})$	$g_1^{I\!R}\,(GeV^{-1})$	$g_2^{I\!R}\,(GeV^{-1})$	$R^2_{0,1}\,(GeV^{-1})$	$G_{3I\!P}\,(GeV^{-1})$
- 0.47	0.0045	0.4	13.5	800	4.0	0.03

- $g_1(b)$ and $g_2(b)$ describe the vertices of interaction of the Pomeron with state 1 and state 2
- The Pomeron trajectory is $1 + \Delta_{I\!P} + \alpha'_{I\!P}$t
- γ denotes the low energy amplitude of the dipole-target interaction
  $G_{3I\!P}$ denotes the triple Pomeron coupling

Comparison of the Energy Dependence of GLM and Experimental Data

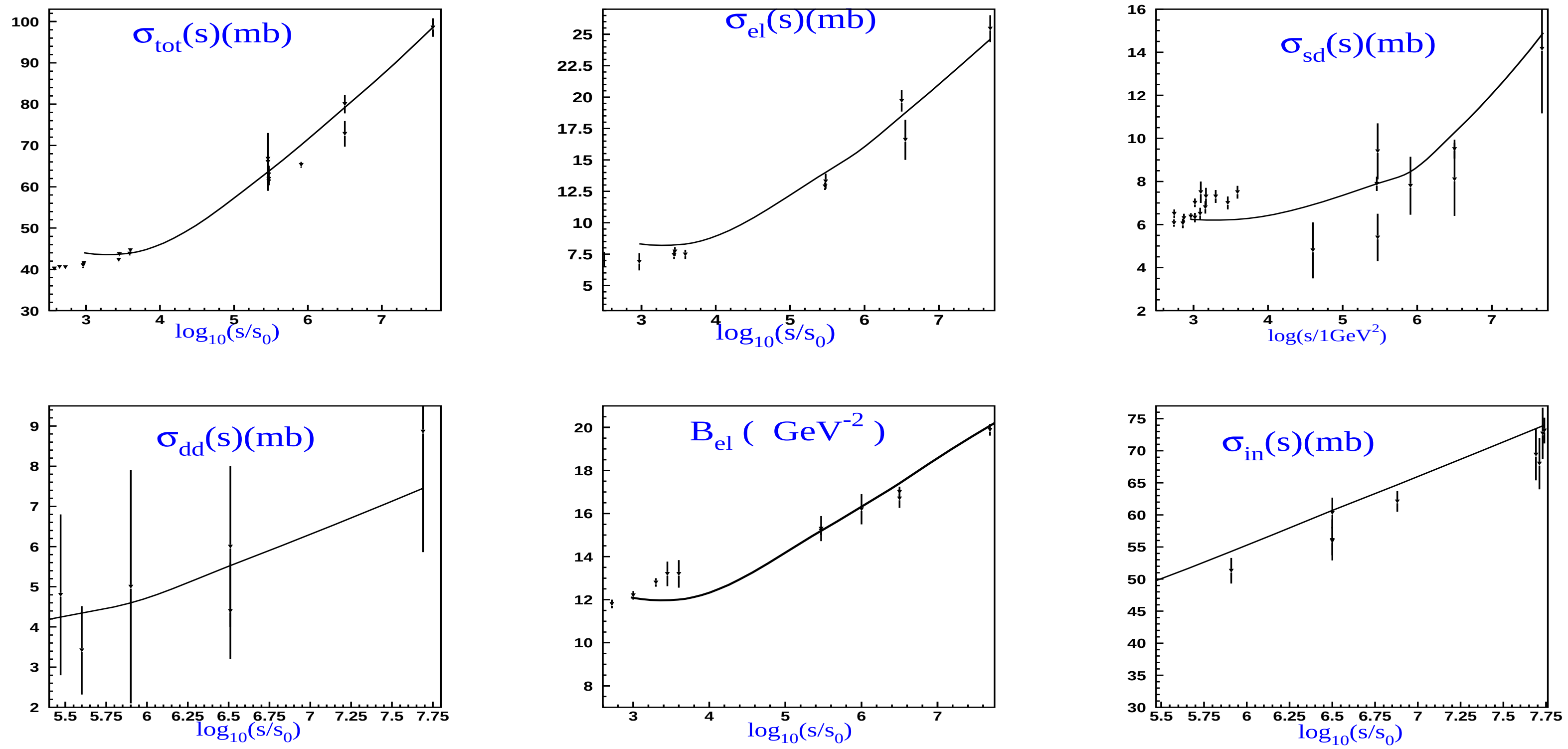

Survival Probability for exclusive central diffractive production of the Higgs boson

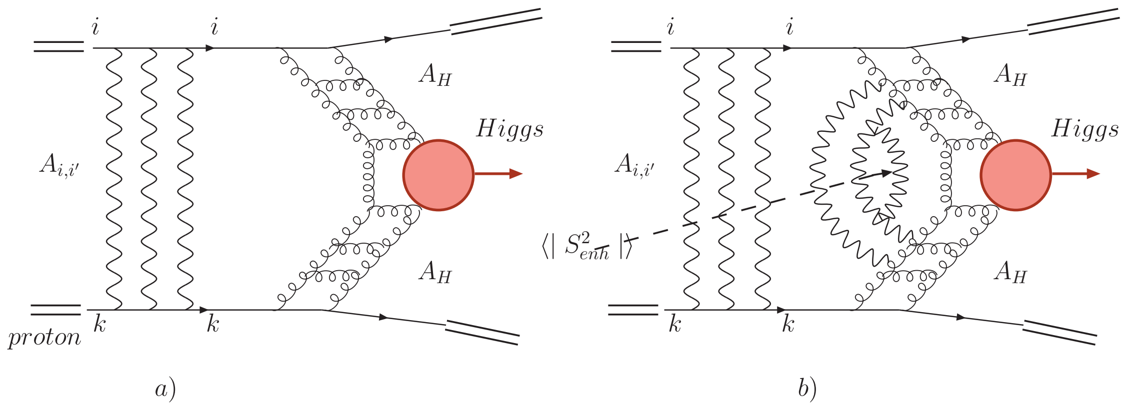

Fig-a shows the contribution to the survival probability in the G-W mechanism

Fig-b illustrates the origin of the additional factor $\langle\mid S^2_{enh}\mid\rangle$

Eikonal s-channel corrections give rise to the LRG survival probability of hard diffraction.

Central Production of Two Hard Jets

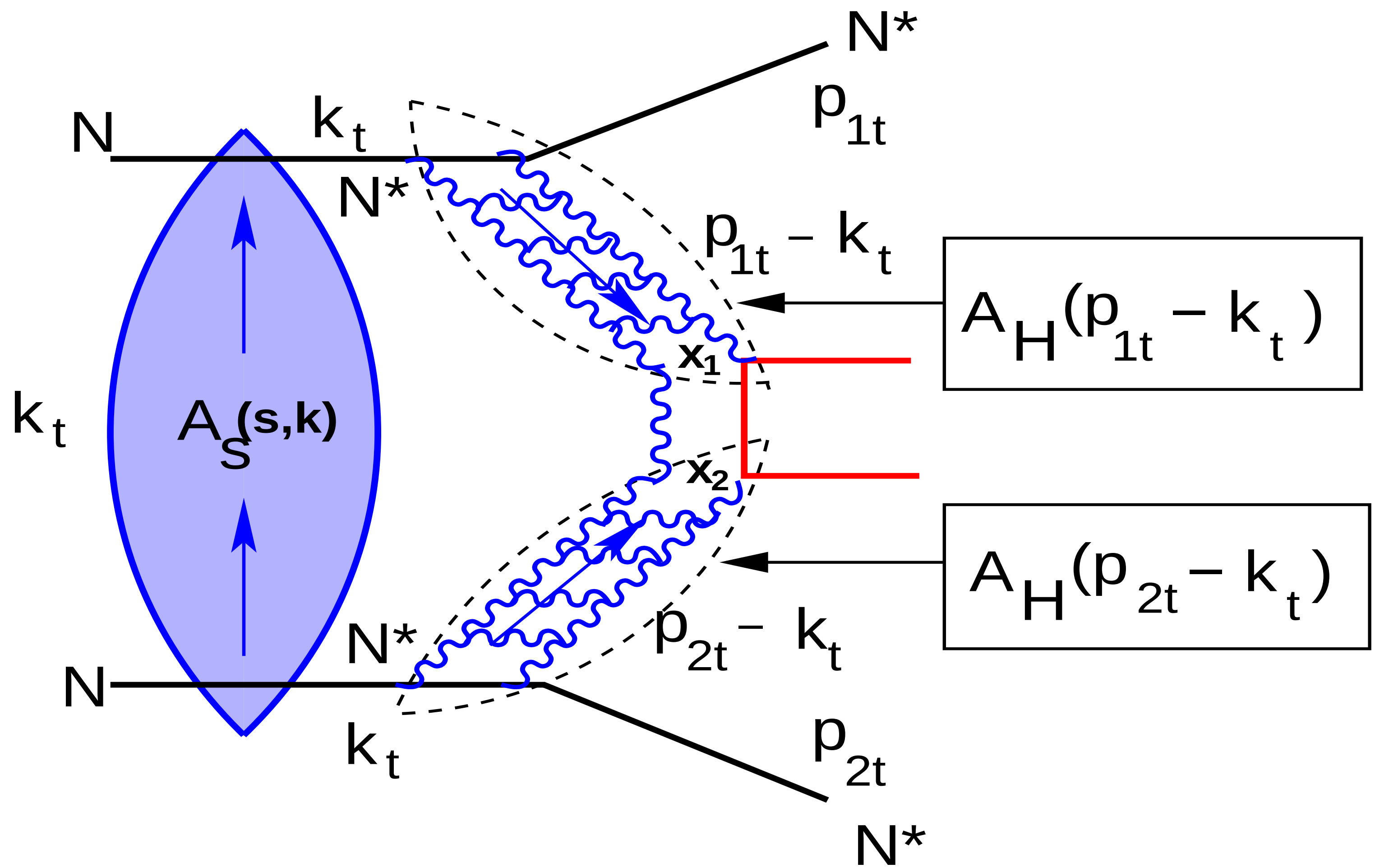

Central production of two hard jets seperated by two large rapidity gaps from the accompaning final state nucleons and/or diffractively exicited states.

Survival Probability of diffractive Higgs production

$$\langle \mid S^2_{2ch} \mid \rangle = \frac{N(s)}{D(s)},$$

where,

$$N(s) = \int d^2\, b_1\, d^2\, b_2 \left[\sum_{i,k} < p|i >^2 < p|k >^2 \;\; A^i_H(s, b_1)\, A^k_H(s, b_2)(1 - A^{i,k}_S\,((s, (\mathbf{b}_1 + \mathbf{b}_2))) \right]^2,$$

$$D(s) = \int\; d^2\, b_1\, d^2\, b_2 \left[\sum_{i,k} < p|i >^2 < p|k >^2 \;\; A^i_H(s, b_1)\, A^k_H(s, b_2) \right]^2.$$

A_s denotes the "soft" strong interaction amplitude.

For the "hard" amplitude $A_H(b,s)$ we assume an input Gaussian b-dependence:

$$A^H_{i,k} = A_H(s)\,\Gamma^H_{i,k}(b)$$

and

$$\Gamma^H_{i,k}(b) = \frac{1}{\pi (R^H_{i,k})^2}\, e^{-\frac{2\,b^2}{(R^H_{i,k})^2}}$$

The "hard" radii are constants determined from HERA data on elastic and inelastic J/Ψ production. We introduce TWO hard b-profiles

$$A^{pp}_H(b) \;=\; \frac{V_{p\to p}}{2\pi B^H_{el}}\exp\left(-\frac{b^2}{2\,B^H_{el}}\right), \qquad and \quad A^{pdif}_H(b) \;=\; \frac{V_{p\to dif}}{2\pi B^H_{in}}\exp\left(-\frac{b^2}{2B^H_{in}}\right).$$

The values B^H_{el}=5.0 GeV^{-2} (?) and B^H_{in}=1 GeV^{-2} have been taken from ZEUS data.

- Contrast to KMR treatment they assume: $A^{pp}_H(b) \;=\; A^{pdif}_H(b) \;\propto\; \exp\left(-\frac{b^2}{2B^H}\right)$
- with $B^H_{el} \;=\; B^H_{inel} = 4\;GeV^{-2}$

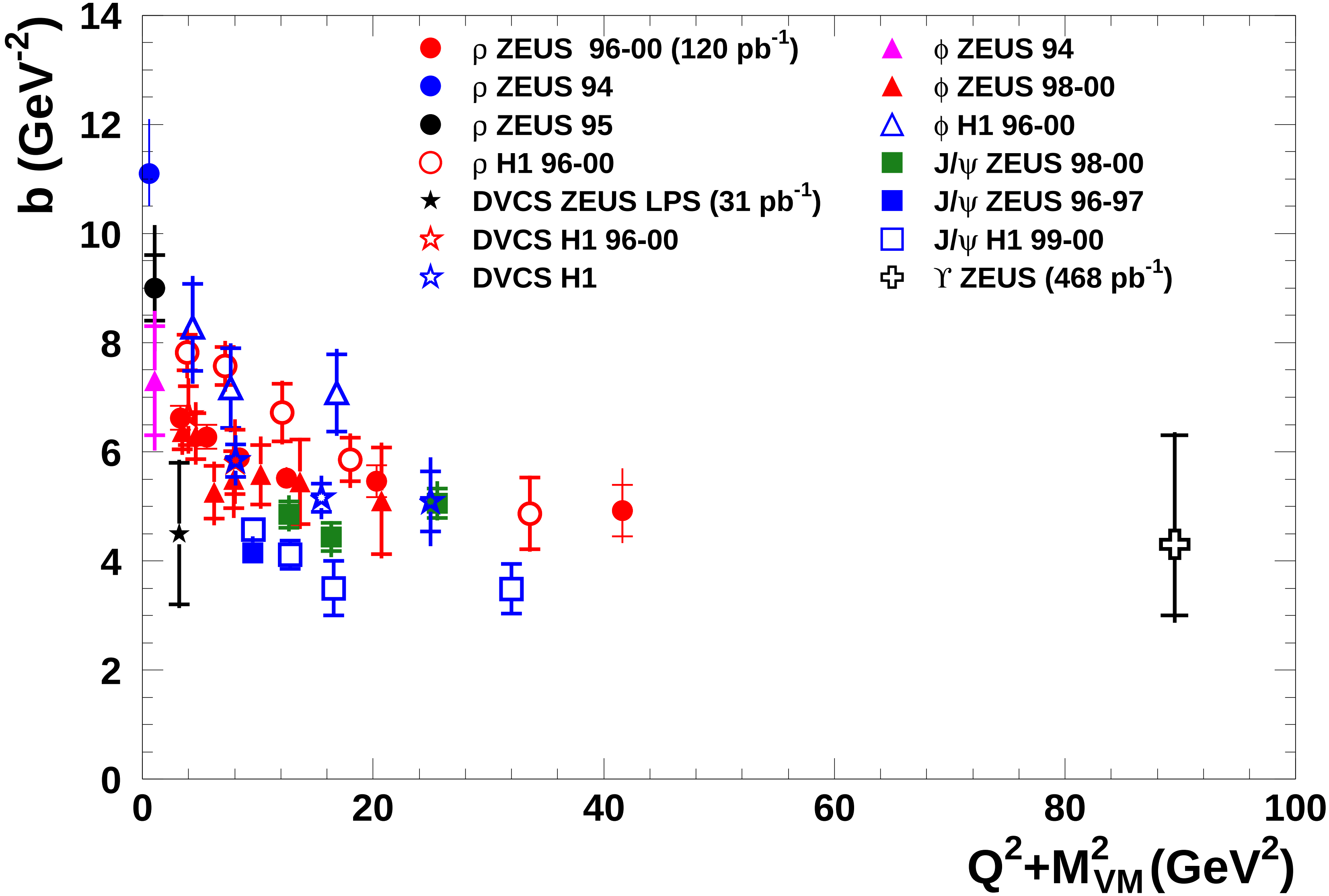
b (GeV^{-2})
14
12
10
8
6
4
2
0
20
40
60
80
100
ρ ZEUS 96-00 (120 pb^{-1})
ρ ZEUS 94
ρ ZEUS 95
ρ H1 96-00
DVCS ZEUS LPS (31 pb^{-1})
DVCS H1 96-00
DVCS H1
ϕ ZEUS 94
ϕ ZEUS 98-00
ϕ H1 96-00
J/ψ ZEUS 98-00
J/ψ ZEUS 96-97
J/ψ H1 99-00
ϒ ZEUS (468 pb^{-1})
$Q^2+M^2_{VM}$ (GeV^2)

The dependence of $< |S^2| >$ at the LHC on B^H_{el} and B^H_{in}

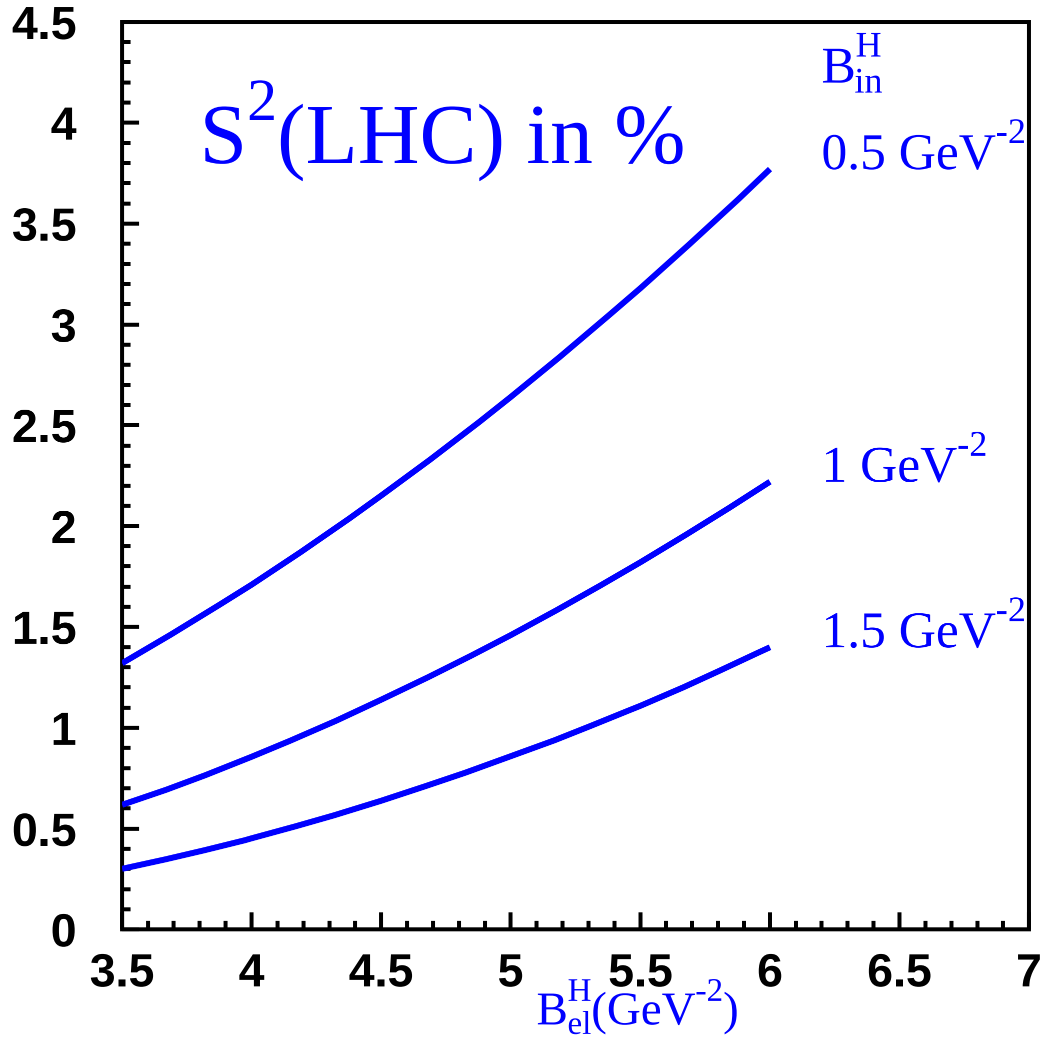

Other results for $< |S^2| >$,

Calculations based on L.O. QCD by Bartels, Bondarenko, Kuta and Motyka [P.R.,D73,093004 (2006)] find for W $=$ 14 TeV

$$S^2_{(TPF)} \;=\; 0.024$$

They have also calculated corrections for hard rescattering which depend on the value taken for α_s.

Frankfurt, Hyde, Strikman and Weiss [P.R.,D75,054009 (2007)] in a partonic approach,
have used a mean field approximation (independent hard and soft scattering).

They find that at LHC energies absorptive interactions of hard spectator partons associated with the process $g + g \to H$, reach the black disc region (for W $> \sqrt{2}$ TeV) and cause additional suppression.

Their result for W $=$ 14 TeV is $< |S^2| > \; = 0.027$
(with a hard slope $B_g \;=\; 3.24\, GeV^{-2}$)

Other results for $< |S^2| >$, contd.

The Durham group (Khoze, Martin and Ryskin) [Eur.Phys.J.C71(2011)71], have a model for soft interactions similar in spirit to GLM. Recently they have improved their model to include a mechanism which mimics BFKL diffusion in k_t. This has now been incorporated into a Monte Carlo generator SuperCHIC.

Their result for the "favored parametrization" for W = 14 TeV, is $\langle |S^2| \rangle = 0.015$

Block and Halzen [Phys.Rev.D73(2006)054022] and Godbole,Grau,Pancheri and Srivastava [Phys.Rev.D72(2005)076001], have obtained estimates for $\langle |S^2| \rangle$, ONLY considering the elastic channels.
(at the Tevatron (W =1800 GeV),$\frac{\sigma_{sd}+\sigma_{dd}}{\sigma_{el}} \approx$ 0.9)

BH quote values: W = 1.8 TeV $\langle |S^2| \rangle = 0.2$
W = 14 TeV $\langle |S^2| \rangle = 0.126$

GGPS find that for W = 14 TeV $\langle |S^2| \rangle$ is 0.05 - 0.1 .

Models neglecting diffractive channels, appear to give too large estimates of $\langle |S^2| \rangle$.

GLM and KMR results for $< S^2 > (\%)$

W (TeV)	GLM	GLM	KMR
	$B_H = 5\ GeV^{-2}$	$B_H = 4\ GeV^{-2}$	$B_H = 4\ GeV^{-2}$
0.63	11.7	9.14	
1.8	7.02	5.12	6.0
7	2.98	1.94	2.4
8	2.7	1.74	
14	1.75	1.07	1.5

At W $=$ 14 TeV; FHSW calculate $< S^2 > (\%) = 2.4$

BBKM find find $< S^2 > (\%) = 2.7$

Conclusions

- Soft scattering sector: Models are compatible.
- Hard production process: sensitive to values of parameters, "Hard slope" etc.
- My estimation is that results for $< |S^2| >$ have an uncertainty of at least 50%.
- Suprizing that completely different approaches
  A) Partonic e.g. BBKM and FHSW

  B) RFT e.g. KMR and GLM

  yield results for $< |S^2| >$ that are so close.

Results of GLM model

$\sqrt{s}$ TeV	1.8	7	8
σ_{tot} mb	79.2	98.6	101.
σ_{el} mb	18.5	24.6	25.2
$\sigma_{sd}(M \leq M_0)$ mb		$10.7 + (2.8)^{nGW}$	$10.9 + (2.89)^{nGW}$
$\sigma_{sd}(M^2 < 0.05s) mb$	$9.2 + (1.95)^{nGW}$	$10.7 + (4.18)^{nGW}$	$10.9 + (4.3)^{nGW}$
σ_{dd} mb	$5.12 + (0.38)^{nGW}$	$6.2 + (1.166)^{nGW}$	$6.32 + (1.29)^{nGW}$
$B_{el}\ GeV^{-2}$	17.4	20.2	20.4
$B_{sd}^{GW}\ GeV^{-2}$	6.36	8.01	8.15
σ_{inel} mb	60.7	74.	75.6
$\frac{d\sigma}{dt}\|_{t=0}\ mb/GeV^2$	326.34	506.4	530.7

$\sqrt{s}$ TeV	14	57
σ_{tot} mb	109.0	130.0
σ_{el} mb	27.9	34.8
$\sigma_{sd}(M^2 < 0.05s)$ mb	$11.5 + (5.81)^{nGW}$	$13.0 + (8.68)^{nGW}$
σ_{dd} mb	$6.78 + (1.59)^{nGW}$	$7.95 + (5.19)^{nGW}$
$B_{el}\ GeV^{-2}$	21.6	24.6
σ_{inel} mb	81.1	95.2
$\frac{d\sigma}{dt}\|_{t=0}\ mb/GeV^2$	608.11	879.2

Predictions of our model for different energies W. M_0 is taken to be equal to $200 GeV$ as ALICE measured the cross section of the diffraction production with this restriction.

Comparison of the results of GLM model and data at 7 and 57 TeV

W	σ_{tot}^{model}(mb)	σ_{tot}^{exp}(mb)	σ_{el}^{model}(mb)	σ_{el}^{exp}(mb)
7 TeV	98.6	TOTEM: 98.6 $\pm$2.2	24.6	TOTEM: 25.4$\pm$1.1

W	$\sigma_{in}^{model}(mb)$	σ_{in}^{exp}(mb)	$B_{el}^{model}(GeV^{-2})$	$B_{el}^{exp}(GeV^{-2})$
7 TeV	74.0	CMS: 68.0$\pm 2^{syst} \pm 2.4^{lumi} \pm 4^{extrap}$ ATLAS: 69.4$\pm 2.4^{exp} \pm 6.9^{extrap}$ ALICE: 73.2 $(+2./-4.6)^{model} \pm 2.6^{lumi}$ TOTEM: 73.5 $\pm 0.6^{stat} \pm 1.8^{syst}$	20.2	TOTEM: 19.9$\pm$0.3

W	$\sigma_{sd}^{model}(mb)$	σ_{sd}^{exp}(mb)	σ_{dd}^{model}(mb)	σ_{dd}^{exp}(mb)
7 TeV	$10.7^{GW} + 4.18^{nGW}$	ALICE : 14.9(+3.4/-5.9)	$6.21^{GW} + 1.24^{nGW}$	ALICE: 9.0 $\pm$ 2.6

W	σ_{tot}^{model}(mb)	σ_{tot}^{exp}(mb)
57 TeV	130	AUGER*: 133 $\pm 13^{stat} \pm 17^{sys} \pm 16^{Glauber}$
	σ_{inel}^{model}(mb)	σ_{inel}^{exp}(mb)
	95.2	AUGER*: 92 $\pm 7^{stat} \pm 11^{syst} \pm 7^{Glauber}$

*AUGER collaboration Phys.Rev.Lett.109,062002 (20112)

GLM Differential cross section and Experimental Data at 1.8 and 7 TeV

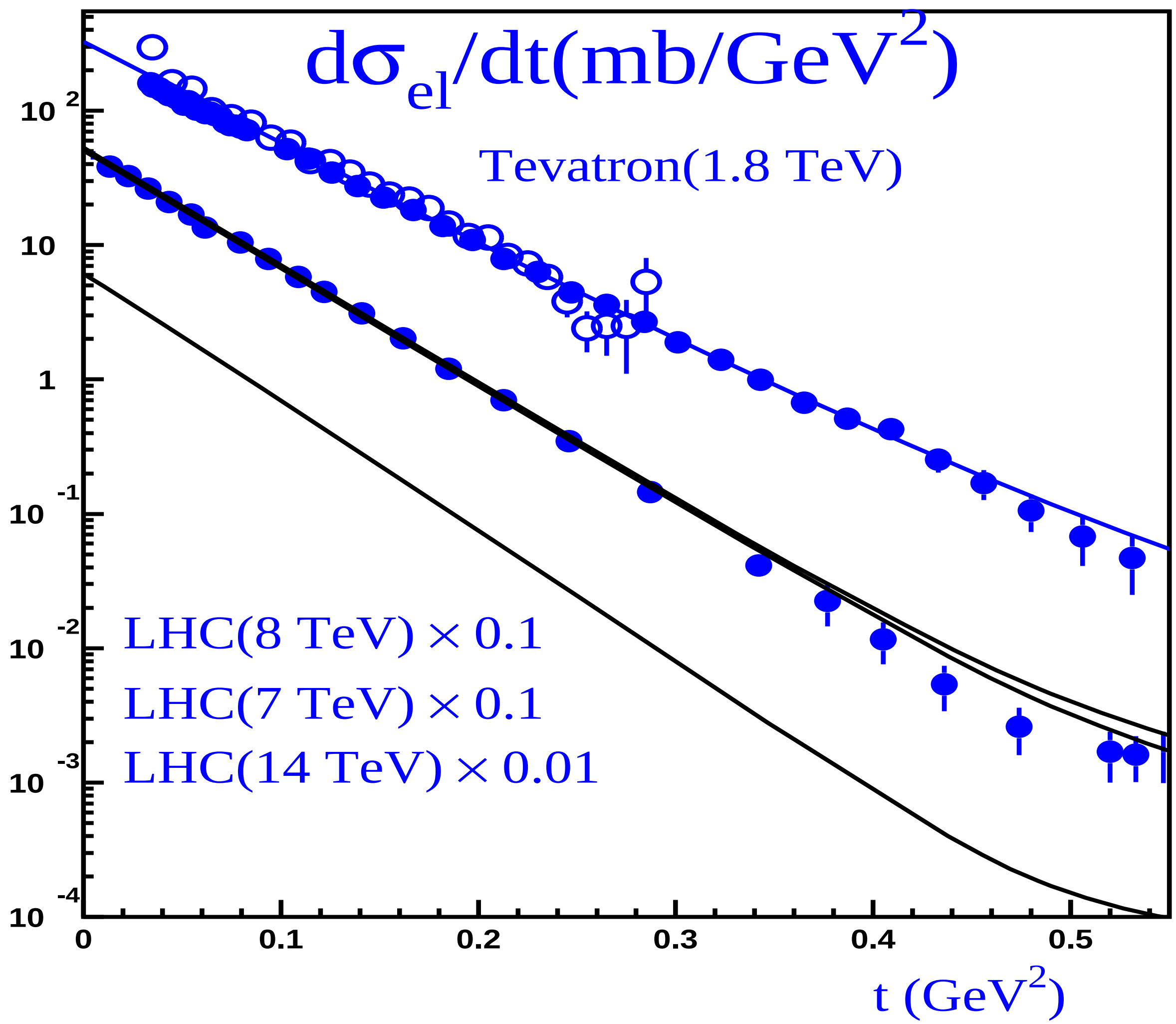

$d\sigma_{el}/dt$ versus $|t|$ at Tevatron (blue curve and data)) and LHC (black curve and data) energies ($W = 1.8\,TeV$, $8\,TeV$ and $7\,TeV$ respectively) The solid line without data shows our prediction for $W = 14\,TeV$.

Good-Walker Formalism

The Good-Walker (G-W) formalism, considers the diffractively produced hadrons as a single hadronic state described by the wave function Ψ_D, which is orthonormal to the wave function Ψ_h of the incoming hadron (proton in the case of interest) i.e. $< \Psi_h | \Psi_D >= 0$.

One introduces two wave functions ψ_1 and ψ_2 that diagonalize the 2x2 interaction matrix $\mathbf{T}$

$$A_{i,k} =< \psi_i \, \psi_k | \mathbf{T} | \psi_{i'} \, \psi_{k'} >= A_{i,k} \, \delta_{i,i'} \, \delta_{k,k'}.$$

In this representation the observed states are written in the form

$$\psi_h = \alpha \, \psi_1 + \beta \, \psi_2 \,,$$
$$\psi_D = -\beta \, \psi_1 + \alpha \, \psi_2$$

where, $\alpha^2 + \beta^2 = 1$

Good-Walker Formalism-2

The s-channel Unitarity constraints for (i,k) are analogous to the single channel equation:

$$Im\, A_{i,k}\,(s,b) = |A_{i,k}\,(s,b)\,|^2 + G^{in}_{i,k}(s,b),$$

$G^{in}_{i,k}$ is the summed probability for all non-G-W inelastic processes, including non-G-W "high mass diffraction" induced by multi-$I\!\!P$ interactions.

A simple solution to the above equation is:

$$A_{i,k}(s,b) = i\left(1-\exp\left(-\frac{\Omega_{i,k}(s,b)}{2}\right)\right), G^{in}_{i,k}(s,b) = 1-\exp\left(-\Omega_{i,k}(s,b)\right).$$

The opacities $\Omega_{i,k}$ are real, determined by the Born input.

Good-Walker Formalism-3

Amplitudes in two channel formalism are:

$$a_{el}(s,b) = i\{\alpha^4 A_{1,1} + 2\alpha^2\beta^2 A_{1,2} + \beta^4 A_{2,2}\},$$

$$a_{sd}(s,b) = i\alpha\beta\{-\alpha^2 A_{1,1} + (\alpha^2 - \beta^2)A_{1,2} + \beta^2 A_{2,2}\},$$

$$a_{dd}(s,b) = i\alpha^2\beta^2\{A_{1,1} - 2A_{1,2} + A_{2,2}\}.$$

With the G-W mechanism σ_{el} , σ_{sd} and σ_{dd} occur due to elastic scattering of ψ_1 and ψ_2, the correct degrees of freedom.